

Multivariate Spectral Analysis of Electroencephalography Data

Claudia Lainscsek^{1,2}, Manuel E. Hernandez^{1,2}, Howard Poizner^{2,3}, and Terrence J. Sejnowski^{1,2}

Abstract—We propose a time-domain approach to detect cross-trial frequencies based on nonlinear correlation functions. This method is a multivariate extension of discrete Fourier transform (DFT) and can be applied to short and/or sparse time series. Cross-trial and/or cross-channel spectra (CTS) can be obtained for electroencephalography (EEG) data where multiple short data segments of the same experiment are available. There are two versions of CTS: The first one assumes some phase coherency across the trials while the second one is independent of phase coherency. We demonstrate that the phase dependent version is more consistent with traditional spectral methods as implemented in EEGLAB. This multivariate spectral analysis is a spatio-temporal extension of DFT and should not be confused with cross-spectral analysis.

We applied this method to EEG data recorded while participants reached for and grasped a virtual object where we compared a cross-trial spectrogram (CTS) of data around a stimulus with traditional event related spectral perturbations (ERSP) analysis. We show that CTS can be applied to shorter data windows than ERSP by using spatio-temporal information in the EEG and therefore yields higher temporal resolution. Furthermore a CTS can be computed for each individual subject while ERSP is commonly computed on a whole population of subjects.

I. INTRODUCTION

The relationship between frequency analysis and analysis of frequency and/or phase couplings in the time domain is poorly understood (see e.g. [1], [2], [3], [4], [5]). In a recent paper Lainscsek et al. [6] found that the linear delay differential equation

$$\dot{x} = ax_\tau, \quad (1)$$

where $x_\tau = x(t - \tau)$ can be used to detect frequencies in the time domain. This approach can be simplified ([7]) by using the expectation value $\langle x^2 \rangle = \lim_{T \rightarrow \infty} \frac{1}{T} \int_0^T x^2 dt$ of a signal

$$\begin{aligned} x(t) &= \sum_{i=1}^N A_i \cos(\omega_i t + \varphi_i) + D \cos(\Omega t + \phi) \\ &= S + D \cos(\Omega t + \phi). \end{aligned} \quad (2)$$

S is the signal under investigation and $D \cos(\Omega t + \phi)$ is a probing signal. $\langle x^2 \rangle$ has a constant value for frequencies Ω

This work was supported by the Howard Hughes Medical Institute, NSF grant #SMA-1041755, NSF ENG-1137279 (EFRI M3C), NIH grant #2 R01 NS036449, and ONR MURI Award No.: N00014-10-1-0072.

¹ Howard Hughes Medical Institute, Computational Neurobiology Laboratory, The Salk Institute for Biological Studies, La Jolla, CA, USA

² Institute for Neural Computation, University of California at San Diego, La Jolla, CA, USA

³Graduate Program in Neurosciences, University of California, San Diego, La Jolla, CA, USA

that are not contained in the signal S under investigation and for frequencies Ω that are contained in the signal S it is the same constant value plus a term that depends on the amplitude and phase of that frequency. Therefore the function

$$L(\Omega) = \max \left(\langle x^2 \rangle - \langle S^2 \rangle - \frac{1}{2} \right). \quad (3)$$

can be used as frequency detector.

The manuscript is organized as follows: Sec. II introduces the application to real world data, the hardware, and the experimental setup. Sec. III describes the data analysis. Sec. IV is the discussion.

II. MATERIALS AND METHODS

Real world data often contain data segments that cannot be used for the analysis. Artifacts in electroencephalography (EEG) data would be an example. Eq. (3) can also be used for sparse data: For a sparse signal $x(T)$, where T is the vector of times for which the signal is good, the probing signal $B \cos(\Omega T + \phi)$ can be used to detect the spectrum. The same trick can be used when very short segments of data need to be analyzed and there are multiple trials of the same experiment: Consider a signal $x_1(T_1), x_2(T_2), \dots, x_n(T_n)$ where all time series $x_i(T_i)$ are centered around the same event, a stimulus S for EEG data (upper plot in Fig. 1). Then

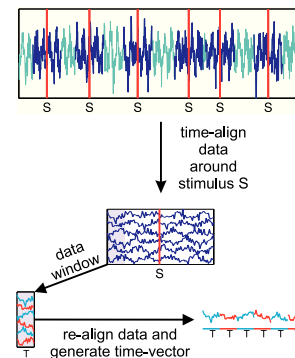


Fig. 1. Re-alignment of data for the computation of a cross-trial spectrogram (CTS) that assumes some phase coherence in the data. First the data are re-aligned around the stimulus S . Then for each data window the data are concatenated and a new time vector is generated. The concatenated data are then the signal S in Eq. (2) and the new time vector is the time in the probing signal.

all time vectors T_i can be considered equal and the signal can be rewritten as $x_1(T), x_2(T), \dots, x_n(T)$ (middle plot in Fig. 1). For a short data window that would be too short

for spectral analysis, the data of all trials can be combined and the spectrum can be computed by using a probing signal with a time vector that consists of n repetitions of the time vector T for n data segments (lower plot in Fig. 1). In this manner cross-trial spectrogram (CTS) can be computed by using sliding short windows. This CTS version assumes phase coherency across the data segments. A cross-trial spectrogram can also be computed in a phase independent manner by computing the spectrum of each time series in the data segment separately using Eq. (3) and then taking the mean over those spectra. In this manuscript we show the differences between the phase dependent and the phase independent versions of the CTS and compare them to traditional methods as implemented in EEGLAB [8]. Cross-trial spectra in the way used here are different from the cross-spectral density ([9], [10], [11]), where the cross-correlation between two signals is used.

We used this method for computing CTS with data windows of only 250 ms length. This corresponds to only 128 data points (the sampling rate was 512 Hz) for each trial. However, when using 50 trials and realigning each data window as shown in Fig. 1, there are then $128 \cdot 50 = 6400$ data points in each data window. We compared this to traditional event related spectral perturbations (ERSP) analysis [12]. The ERSP measures average dynamic changes in amplitude of the broad band EEG frequency spectrum as a function of time relative to an experimental event. To compute an ERSP, baseline spectra are calculated from the EEG immediately preceding each event. The epoch is divided into overlapping data windows and a moving average of the amplitude spectra of these is created. Each of these spectral transforms of individual response epochs are then normalized by dividing by their respective mean baseline spectra. Normalized response transforms for many trials are then averaged to produce an average ERSP.

The main difference between the proposed method of cross-trial spectrograms (CTS) and traditional ERSP analysis is that CTS uses the data of each data window of many trials simultaneously to compute the spectrogram, while ERSP averages over individual spectra. Therefore CTS can use shorter data windows if enough trials are available, and ERSP is restricted to the minimum window length for each spectrum.

A. Hardware

Electroencephalographic (EEG) data were collected using a 70-channel active electrode EEG system (Biosemi Inc. ActiveTwo, Amsterdam, Netherlands) consisting of a cap plus four EOG electrodes, temporal to both eyes and above and below the right eye, two EMG electrodes on the trapezius and right and left sternocleidomastoids, and two reference electrodes on the left and right mastoids. Data were recorded with a 512 Hz sampling rate, and referenced to the averaged mastoid electrodes. Head position relative to the EEG sensors was determined with a electromagnetic

motion tracking system (Polhemus, FASTRAK, Colchester, VT, USA).

B. Participants

Nine healthy older adults (4 females) participated in this study (mean \pm SD age: 64.3 ± 7.9 years). No participant had any neurological or psychiatric disease. All participants were right-hand dominant with normal or corrected to normal vision. All participants signed the informed consent document approved by the human subjects Institutional Review Board of the University of California, San Diego.

C. Protocol

Participants reached for and grasped a virtual rectangular object (3.5 x 8.5 x 6 cm) with haptic feedback provided to the thumb and index finger by two 3-degree of freedom haptic robotic devices (Phantom Premium 1.0, Geomagic, Wilmington, MA, USA). Participants placed the digits of their right hand on a virtual starting dock and a the sound of a tone reached for the object at a comfortable speed. The object was located 13-18 cm away in a virtual environment designed using custom scripts (Vizard, WorldViz LLC, Santa Barbara, CA, USA, [13]). Participants were provided haptic as well as visual feedback of the dock so that they felt their hands resting on a solid surface. Overall, a maximum of 360 (10 blocks of 36 trials) trials were performed by each participant, with rest provided between blocks to limit fatigue. In this study, we considered EEG data from 50 randomly selected trials from -1.5 seconds before the tone stimulus (S) to 1.5 seconds after the stimulus.

III. DATA PROCESSING AND ANALYSIS

We analyzed two sets of data, raw and clean data. To get clean data, raw EEG data were imported into EEGLAB using MATLAB (The MathWorks, Natick, MA, USA) for processing [8]. Data were high-pass filtered at 1 Hz to remove drift and low-pass filtered at 55 Hz to remove line noise. EEG artifacts associated with eye and other muscle movement were removed using independent component analysis (ICA) [14]. Based on the topography, spectra, and trial-to-trial characteristics of ICA components, non-artifactual components were selected and used to generate

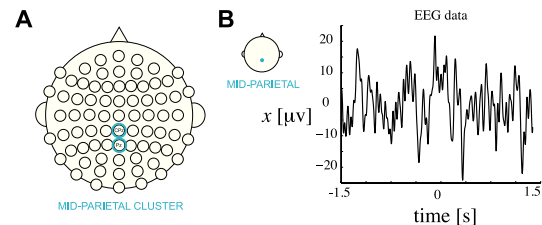


Fig. 2. (A) Mid-parietal EEG cluster containing the Pz and CPz electrodes used in this analysis. (B) Sample EEG time series.

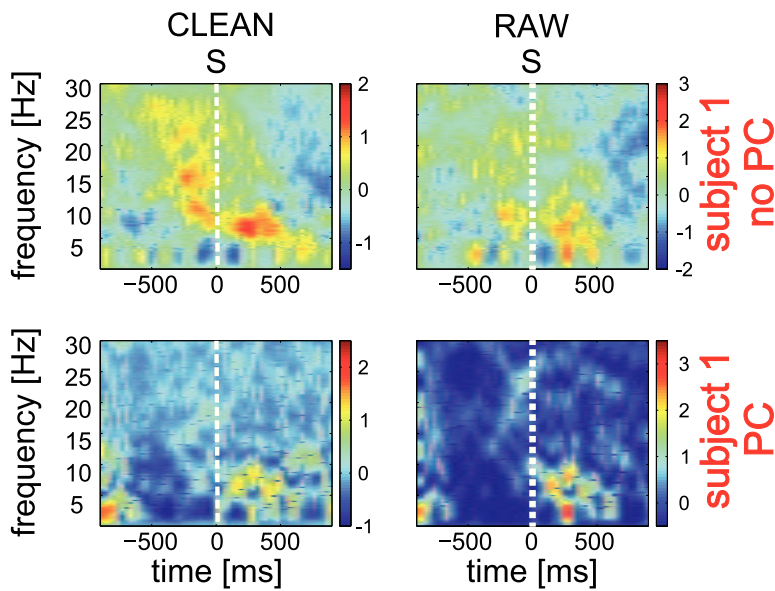


Fig. 3. Cross-trial spectrograms of 50 randomly selected trials time-locked to a stimuli onset (dashed white lines) in a single participant. The dominant frequencies detected in clean EEG data are consistent with the raw EEG data. The lower two plots use the CTS that assumes phase coherency (PC) and the upper plots use the phase independent CTS (no PC). The upper two plots are more consistent with the traditional ERSP analysis (see upper two plots in Fig. 4)

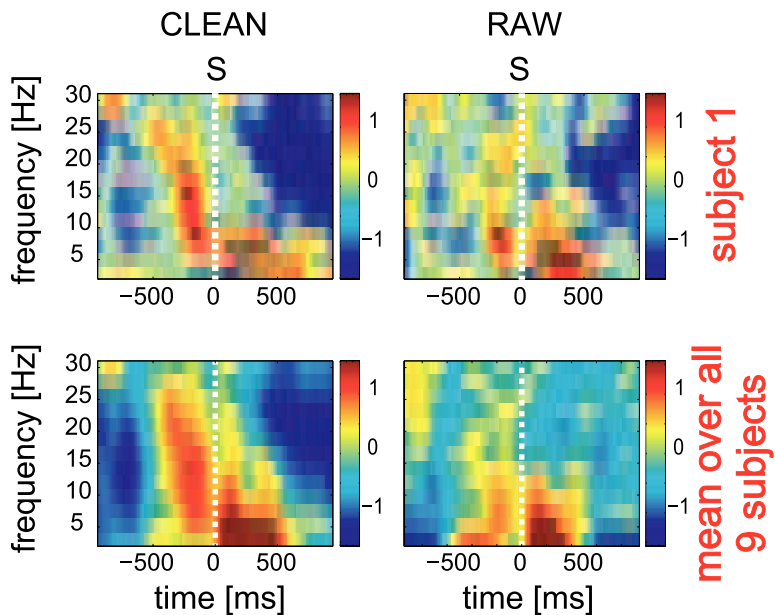


Fig. 4. ERSP analysis on the same subject as used in Fig. 3 (upper plots) and mean over all nine subjects (lower plots). The ERSP analysis demonstrates increased low frequency and decreased high frequency activity after the stimuli (S) in clean EEG data recorded over the mid-parietal cluster, and the increased low frequency activity prior to the stimuli in raw EEG data.

back-projected EEG data, which will be referred to as clean EEG.

The re-arranged EEG data (see Fig. 1) from a central parietal region consisting of electrodes Pz and CPz were used for the cross-trial time domain frequency analysis. These mid-parietal electrodes were selected due to the critical role of the parietal cortex in online reaching and

grasping [15], [16] (Fig. 2). The raw and clean data were analyzed using 1/4 second sliding time windows with an overlap of 1/32 s and a probing frequency signal ranging from 0.5 to 30 Hz. Fig. 3 shows both versions of the obtained CTS. The upper two plots show the phase dependent CTS that assumes phase coherency (PC) while the lower plots show the phase independent CTS (no PC).

For comparison to this novel cross-trial frequency analysis methods, event-related spectral perturbations (ERSPs) were calculated for the mid-parietal cluster using Morlet wavelets (or Gabor wavelets [17], [18], [19], [20]). We used the EEGLAB default parameters (200 time point windows) and all 50 trials from the nine participants. Fig. 4 shows the ERSP plots on clean and raw EEG data. We found that, consistent with ERSP analysis (Fig. 4), the go tone elicited an increase in low-frequency neural activity in the delta (0.5 to 4 Hz), theta (4 to 8 Hz), and alpha (8-12 Hz) bands (Fig. 5). In the raw data, there was an increase in delta activity approximately 500 ms before the tone, which is also noticeable in the cross-spectrum analysis. Clean and raw EEG data demonstrate similarities in the dominant frequencies detected in the signal, particularly in the lower frequencies (Fig. 5). Prior to tone onset, we found

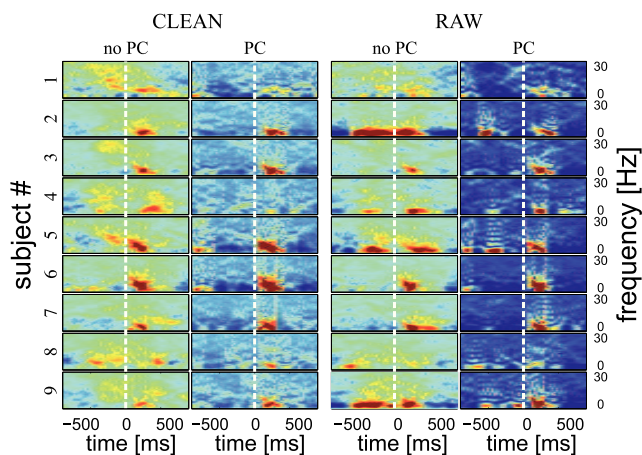


Fig. 5. Cross-trial spectrogram of clean and raw EEG data in all nine participants. Increased amplitudes are observed in the lower frequency bands after the go tone in both clean and raw EEG data. The phase dependent (no PC) and phase independent (PC) versions of the CTS are shown in separate columns for the clean as well as the raw data.

an increase in beta frequency (13-30 Hz), and subsequent decrease in beta frequency content during movement.

IV. DISCUSSION

We demonstrate that CTS analysis seems to be able to distinguish changes in frequency in a broad-band physiological signal, even without any pre-processing using only sparse, short time segments. Data cleanup using ICA does not significantly alter the dominant frequencies in the spectrograms compared to using raw data (see Fig. 5). In contrast to traditional ERSP analysis, the current CTS analysis is capable of using shorter data windows and thus allows for finer identification of frequencies in an EEG signal. However, further work remains to assess the sensitivity of this method on broad-band systems, and similarities and contrasts to other existing frequency analysis methods. This time domain frequency analysis tool appears to be very promising for use in future applications of noisy and

complex signals, such as EEG, where a measure of rapid changes in frequency is desired.

ACKNOWLEDGMENT

We would like to thank Jonathan Weyhenmeyer for discussion on this paper.

REFERENCES

- [1] B. Hjorth, "EEG analysis based on time domain properties," *Electroencephalography and Clinical Neurophysiology*, vol. 29, no. 3, pp. 306 – 310, 1970.
- [2] Y. Chan and R. Langford, "Spectral estimation via the high-order yule-walker equations," *Acoustics, Speech and Signal Processing, IEEE Transactions on*, vol. 30, no. 5, pp. 689 – 698, 1982.
- [3] M. Raghuvver and C. Nikiias, "Bispectrum estimation: A parametric approach," *Acoustics, Speech and Signal Processing, IEEE Transactions on*, vol. 33, no. 5, pp. 1213 – 1230, 1985.
- [4] M. R. Raghuvver and C. L. Nikiias, "Bispectrum estimation via AR modeling," *Signal Processing*, vol. 10, no. 1, pp. 35 – 48, 1986.
- [5] L. Stankovic, "A method for time-frequency analysis," *Signal Processing, IEEE Transactions on*, vol. 42, no. 1, pp. 225 –229, jan 1994.
- [6] C. Lainscsek and T. Sejnowski, "Electrocardiogram classification using delay differential equations," *Chaos*, vol. 23(2), p. 023132, 2013.
- [7] —, "Time domain frequency analysis and higher order statistics," *Physical Review Letters*, 2013, in review.
- [8] A. Delorme and S. Makeig, "EEGLAB: an open source toolbox for analysis of single-trial EEG dynamics including independent component analysis," *J Neurosci Methods*, vol. 134, no. 1, pp. 9–21, 2004.
- [9] R. Bracewell, *The Fourier Transform and Its Applications*. New York: McGraw-Hill, 1965, ch. Pentagram Notation for Cross Correlation., p. 46 and 243.
- [10] A. Papoulis, *The Fourier Integral and Its Applications*. New York: McGraw-Hill, 1962, pp. 244–245 and 252–253.
- [11] [Online]. Available: <http://www.mathworks.com/help/signal/ref/cpsd.html>
- [12] S. Makeig, "Auditory event-related dynamics of the EEG spectrum and effects of exposure to tones," *Electroencephalography and Clinical Neurophysiology*, vol. 86, p. 283, 1993.
- [13] J. Snider, M. Plank, D. Lee, and H. Poizner, "Simultaneous neural and movement recordings in large-scale immersive virtual environments," *IEEE Transactions on Biomedical Circuits and Systems*, 2013.
- [14] T. Jung, S. Makeig, C. Humphries, T. Lee, M. McKeown, V. Iragui, and T. Sejnowski, "Removing electroencephalographic artifacts by blind source separation," *Psychophysiology*, vol. 37, no. 2, pp. 163–78, 2000.
- [15] C. Buneo and A. R.A., "The posterior parietal cortex: sensorimotor interface for the planning and online control of visually guided movements," *Neuropsychologia*, vol. 44(13), pp. 2594–606, 2006.
- [16] E. Tunik, S. Ortigue, S. Adamovich, and S. Grafton, "Differential recruitment of anterior intraparietal sulcus and superior parietal lobule during visually guided grasping revealed by electrical neuroimaging," *J. Neurosci.*, 2008.
- [17] A. Goupillaud, P. Grossman and J. Morlet, "Cycle-octave and related transforms in seismic signal analysis," *Geoexploration*, vol. 23, pp. 85–102, 1984.
- [18] N. Delprat, B. Escudie, P. Guillemain, R. Kronland-Martinet, P. Tchamitchian, and B. Torresani, "Asymptotic wavelet and gabor analysis: extraction of instantaneous frequencies," *Information Theory, IEEE Transactions on*, vol. 38, no. 2, pp. 644–664, 1992.
- [19] A. Bernardino and J. Santos-Victor, "A real-time gabor primal sketch for visual attention;" in *Pattern Recognition and Image Analysis*, ser. Lecture Notes in Computer Science, J. Marques, N. Prez de la Blanca, and P. Pina, Eds. Springer Berlin Heidelberg, 2005, vol. 3522, pp. 335–342.
- [20] D. Gabor, "Theory of communication," *J. Inst. Elect. Eng.*, vol. 93(3), p. 429, 1946.